Photon specific absorbed fractions calculated in adult voxel phantoms with the EGS4 and the MCNP4 Monte Carlo codes

R. Kramer[1], H. J. Khoury[1], H. Yoriyaz[2] and F. R. A. Lima[3]

[1]Departamento de Energia Nuclear, UFPE, Recife, PE, Brazil.
E-mail: rkramer@uol.com.br
[2]Instituto de Pesquisas Energéticas e Nucleares, CNEN, São Paulo, Brazil.
[3]Centro Regional de Ciências Nucleares, CNEN, Recife, PE, Brazil.

Abstract. Dose coefficients for intakes of radionuclides published by the International Commission on Radiological Protection (ICRP) are based on specific absorbed fractions (SAFs), which have been calculated in the mathematical MIRD phantoms. The organs of the mathematical phantoms, defined by geometrical bodies, like circular and elliptical cylinders, ellipsoids, cones, tori, etc., serve as rather simple representations of real human body organs. Tomographic or voxel phantoms are based on digital images recorded from scanning of real persons by computed tomography (CT) or magnetic resonance imaging (MRI). Compared to the mathematical MIRD phantoms, voxel phantoms are true to nature representations of the human body. The replacement of the MIRD phantoms by voxel phantoms proposed by the ICRP raises the question about the changes to be expected for the SAFs, and consequently also for the dose coefficients. In order to investigate the dosimetric consequences of this replacement, SAFs have been calculated in the recently introduced MAX (*M*ale *A*dult *voXel*) and FAXht (*F*emale *A*dult *voXel*) head+trunk phantoms for photon energies between 10 keV and 4 MeV. For this purpose the phantoms have been connected to the EGS4 as well as to the MCNP4 code, which at present are probably the most used general-purpose Monte Carlo codes. Thereby it was possible to assess the impact on the SAFs, if different radiation transport methods are used. The mathematical MIRD phantoms have also been connected to the EGS4 code, and their elemental compositions of body tissues were replaced by those used in the voxel phantoms. In this manner it was possible to compare the SAFs of the MIRD phantoms on the one hand and the MAX and FAX phantom on the other hand as a function of the geometrical anatomy only, i.e. the volume, the shape and the position of organs at risk.

1. Introduction

For more than three decades equivalent or absorbed dose estimates from incorporated radionuclides were based on specific absorbed fractions (SAFs), which have been calculated by Monte Carlo methods in so-called 'MIRD phantoms', a serie of adult and pediatric mathematical representations of human bodies. In mathematical human phantoms size and form of the body and its organs are described by mathematical expressions representing combinations and intersections of planes, circular and elliptical cylinders, spheres, cones, tori, etc.

Fisher and Snyder [1, 2] introduced this type of phantom for an adult male which also contains ovaries and a uterus. During the compilation of the Report of the Task Group on Reference Man [3] the phantom has been further developed by Snyder et al [4, 5]. Since then it is known as "MIRD-5 phantom" (*M*edical *I*nternal *R*adiation *D*ose Committee (MIRD) Pamphlet No.5).

The MIRD-5 phantom has been the basis for various derivations representing infants and children of various ages [6], gender-specific phantoms called ADAM and EVA [7] and a pregnant female adult phantom [8]. Body height and weight as well as the organ masses of these MIRD-type phantoms are in accordance with the first set of Reference Man data [3]. Although being rather crude representations of the human body, at the time of their introduction the MIRD-type phantoms represented a significant progress for the assessment of equivalent or absorbed dose to radiosensitive organs of the human body in the areas of radiation protection and nuclear medicine.

In the meantime progress took place in the development of clock-speed and storage capacity of computers, and as a consequence the production and processing of images has been pushed to levels hardly imagined before. These new image capabilities have recently been used to introduce

tomographic or voxel-based phantoms, which overcome the crude representation of the human body by mathematical phantoms. Voxel phantoms are based on digital images recorded from scanning of real persons by computed tomography (CT) or magnetic resonance imaging (MRI). Each image consists of a matrix of pixels (picture elements), whose number depends on the resolution chosen during scanning. A consecutive set of such images can be considered as a three-dimensional matrix made of voxels (volume pixels), where each voxel belongs to a specific organ or tissue. Compared to the mathematical phantoms, voxel phantoms are true to nature representations of the human body.

Based on data published by Zubal [9] on a website of the YALE university, Kramer et al [10] developed the MAX (*M*ale *A*dult *voXel*) phantom, which corresponds anatomically to the specifications of the revised Reference Man Report [11], and in a paper presented at this congress the FAXht (*F*emale *A*dult *voXel*) head+trunk phantom [12] will be described, which corresponds to the anatomical specifications for the Reference Adult Female defined in ICRP89 [11].

This paper will present SAFs for various radiosensitive organs and tissues for the mathematical ADAM and EVA phantoms as well as for the MAX and FAXht phantoms when the liver represents the source organ. The data have been taken from an ongoing investigation which involves many other source and target organs and tissues,and which was motivated by the intention of the ICRP [13] to replace the MIRD-type phantoms by voxel phantoms.

2. Materials and methods

Compared to the exposure models used 25-30 years ago to calculate SAFs, the change intended by the ICRP would not only imply replacing the mathematical by voxel phantoms, but also updating the tissue compositions, and substituting the ALGAM-based Monte Carlo code for photons by modern codes which allow for secondary particle transport, Rayleigh scattering, etc.
In order to show the dosimetric consequences of these changes separately, the following exposure models were used:

a) ADEV/EGS4: The mathematical ADAM and EVA phantoms connected to the EGS4 Monte Carlo code with the original tissue composition from Kramer et al [7].
b) ADEV44/EGS4: The mathematical ADAM and EVA phantoms connected to the EGS4 Monte Carlo code with new tissue compositions taken from ICRU44 [14], with a homogeneous mixture in all skeletal voxels based on ICRP70 [15], and a homogeneous mixture of adipose and muscle in all unspecified regions of the body.
c) MFHOM/EGS4: The MAX and the FAXht phantoms connected to the EGS4 Monte Carlo code with ICRU44 tissue compositions, and with the same homogeneous mixture in all skeletal voxels, and for adipose and muscle in all unspecified regions of the body used for b).
d) MAX/FAXht-EGS4: The MAX and the FAXht phantoms connected to the EGS4 Monte Carlo code with ICRU44 tissue compositions, heterogeneous skeleton and separately segmented regions for adipose and muscle.
e) MAX/MCNP4: The MAX phantom connected to the MCNP4 Monte Carlo code with ICRU44 tissue compositions, heterogeneous skeleton and separately segmented regions for adipose and muscle.

Detailed descriptions of the phantoms used for this study can be found in Kramer et al [7, 10, 16, 28], and in Lima et al [17].

3. Results

3.1 Specific absorbed fractions

Figures 1 to 3 present SAFs for four organs and tissues with the greatest tissue weighting factors based on the concept of effective dose [18], that is the gonads, the lungs, the colon, and the stomach for photon emitters homogeneously distributed in the liver. Figures 1a, 2a, and 3a show data for reference adult males, while Figures 1b, 2b, and 3b present the same quantities for reference adult females.

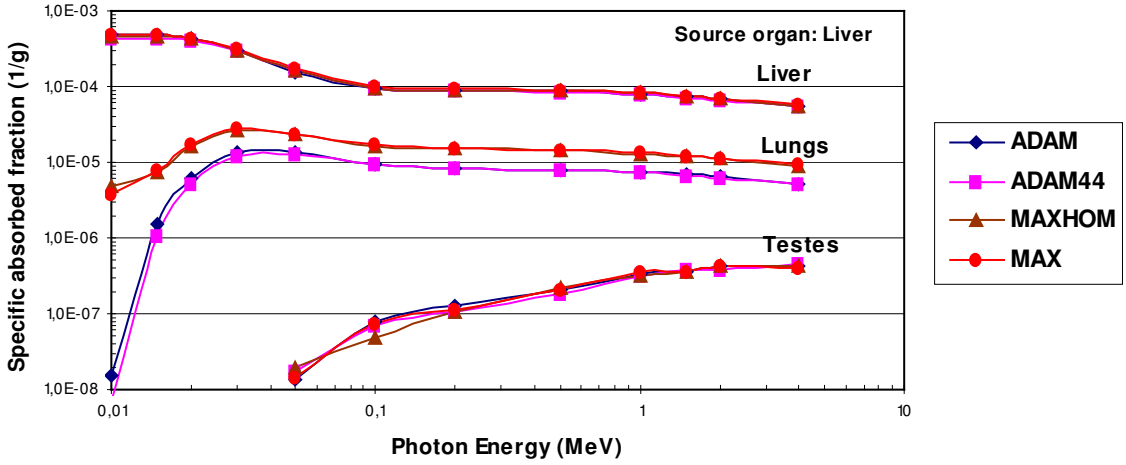

FIG 1a. Male specific absorbed fractions

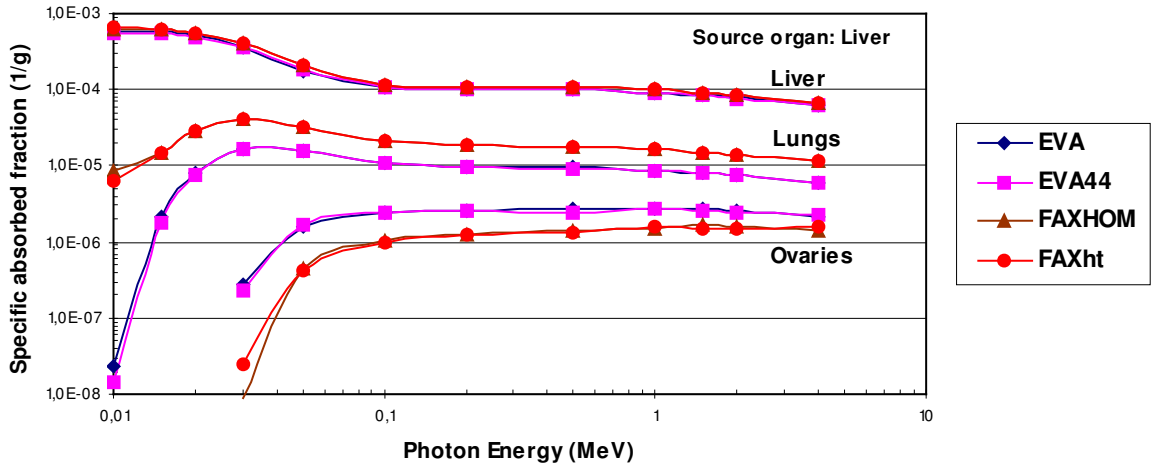

FIG 1b. Female specific absorbed fractions

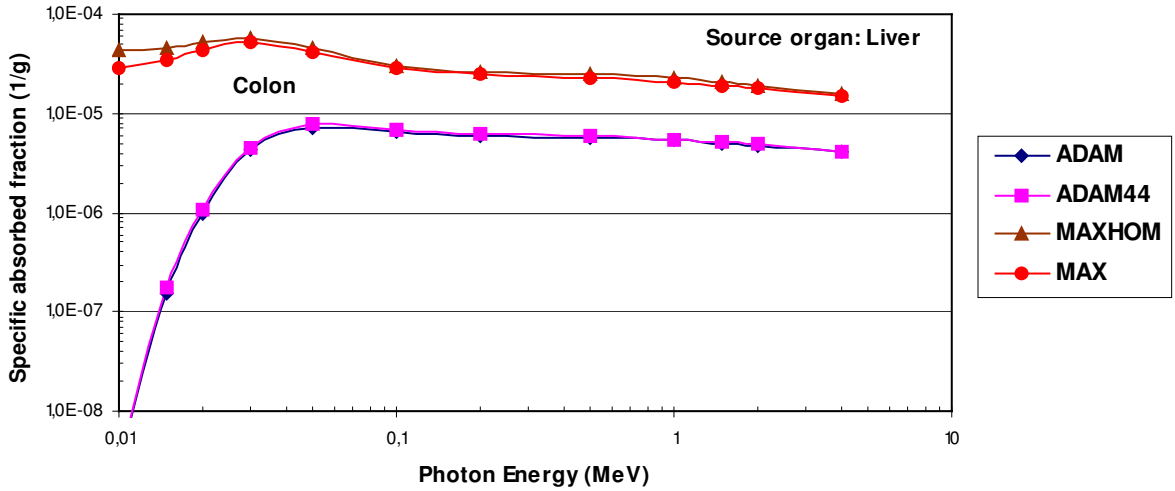

FIG 2a. Male specific absorbed fractions

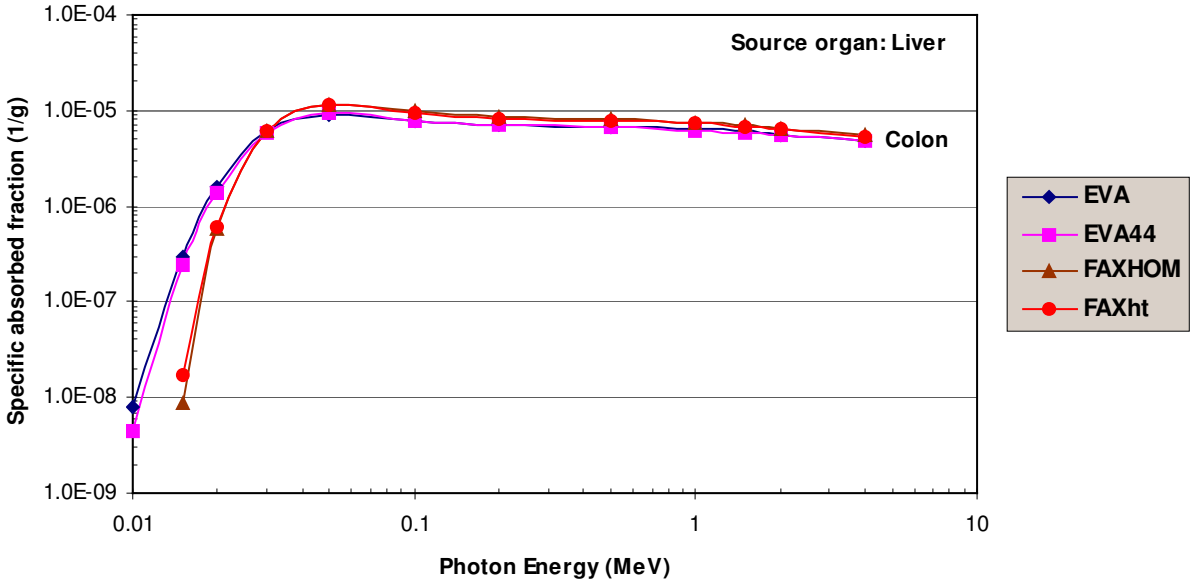

FIG 2b. Female specific absorbed fractions

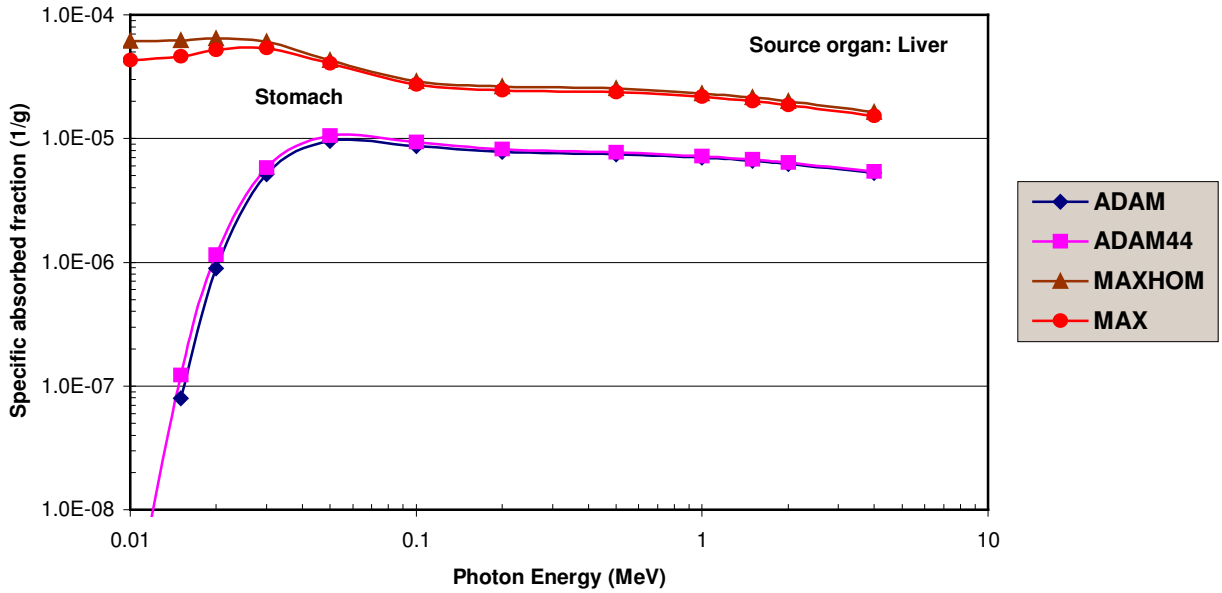

FIG 3a. Male specific absorbed fractions

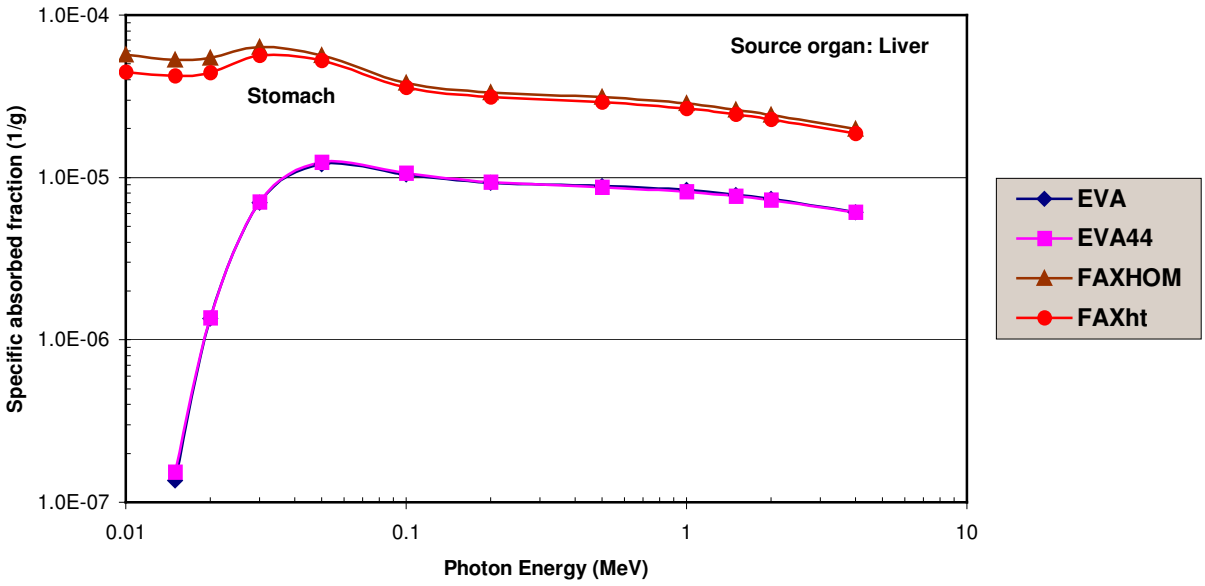

FIG 3b. Female specific absorbed fractions

3.1.1 Tissue composition (a – b)

According to the ratios between the mass-energy absorption coefficients of the old and new tissue compositions shown in Figure 4, the equivalent dose to soft-tissue organs, the bones, and the skin are expected to increase as a result of this change, while the equivalent dose to the lungs would slightly decrease or remain unchanged. The unspecified regions in the body would see a decrease of equivalent dose when soft-tissue is replaced by a homogeneous mixture of adipose and muscle (ADIMUS). The data of Figure 4 were compiled for an investigation on external exposures to photons [16], but they can also serve as an indicator for what is to be expected in the actual study for internal emitters.

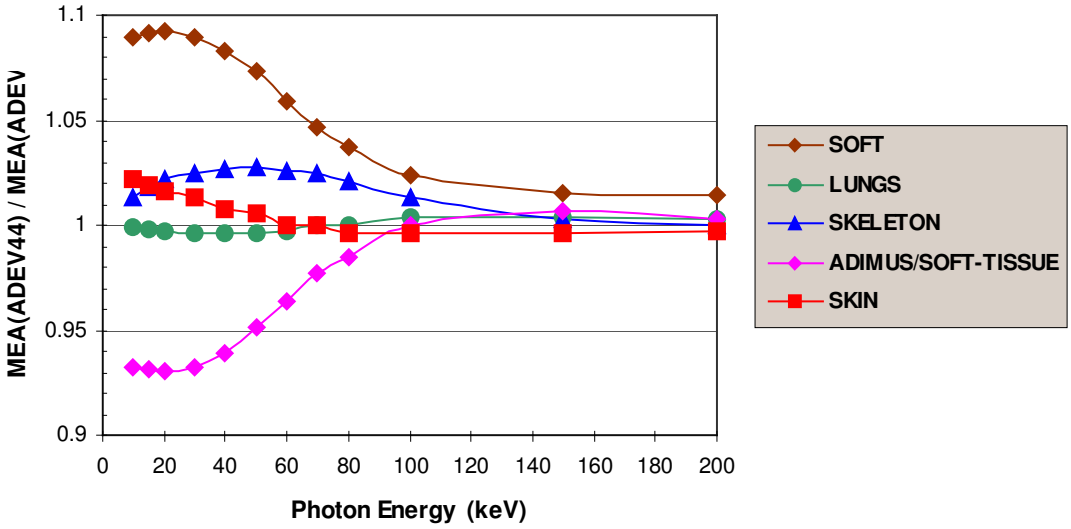

FIG 4. Ratios of mass-energy absorption coefficients

Indeed, most of the SAFs for ADAM44 and EVA44 presented in Figures 1 – 3 show a small increase compared to the SAFs for ADAM and EVA.

3.1.2 Anatomy (b – c)

The introduction of voxel phantoms based on patient data, which usually have shorter inter-organ distances than the mathematical phantoms, leads generally to an increase of the SAFs (Figures 1 to 3), except for the colon and the ovaries of the FAXht phantom. The colon of the FAXht phantom is in a greater distance from the liver compared to the MAX phantom. The same argument holds for the ovaries compared to their position in the EVA phantom. Because of poor statistics it is difficult to identify a clear trend for the testes. Contrary to the findings for external exposures to photons [16], the introduction of voxel phantoms of real persons often increases the exposure to radiosensitive organs and tissues, at least to the gonads, the lungs, the colon, and the stomach as target organs when the liver is the source organ. Future evaluation for other combinations of source and target organs will show if this can be considered as a general aspect for internal exposures.

3.1.3 Heterogeneous skeleton and separately segmented adipose and muscle (c – d)

The introduction of a heterogeneous distribution of skeletal tissues among the bone voxels, and the separately segmented regions for adipose and muscle leads sometimes to a small decrease of the SAFs, or cause no change at all. This substitution actually changes to some extent the "shielding environment" for some of the radiosensitive organs and tissues, but for the combination of source and target organs given no dramatic changes were expected, which is confirmed by the MAX and FAXht SAFs of Figures 1 – 3.

3.1.4 Monte Carlo code (d – e)

Figure 5 shows SAFs calculated with the MAX phantom which was connected to the EGS4 as well as to the MCNP4 Monte Carlo codes. The average differences found between the SAFs are 3.7% for the liver, 11.3% for the lungs, 4.4% for the red bone marrow (RBM), and 12.9% for the testes. The small size and the relatively distant location from the source organ explain the deviation between the two testes SAFs. The agreement between the liver and the RBM SAFs for the two Monte Carlo codes is satisfactory. The SAFs for the lungs show relatively great differences for energies below 50 keV. The explanation for these differences has still to be investigated.

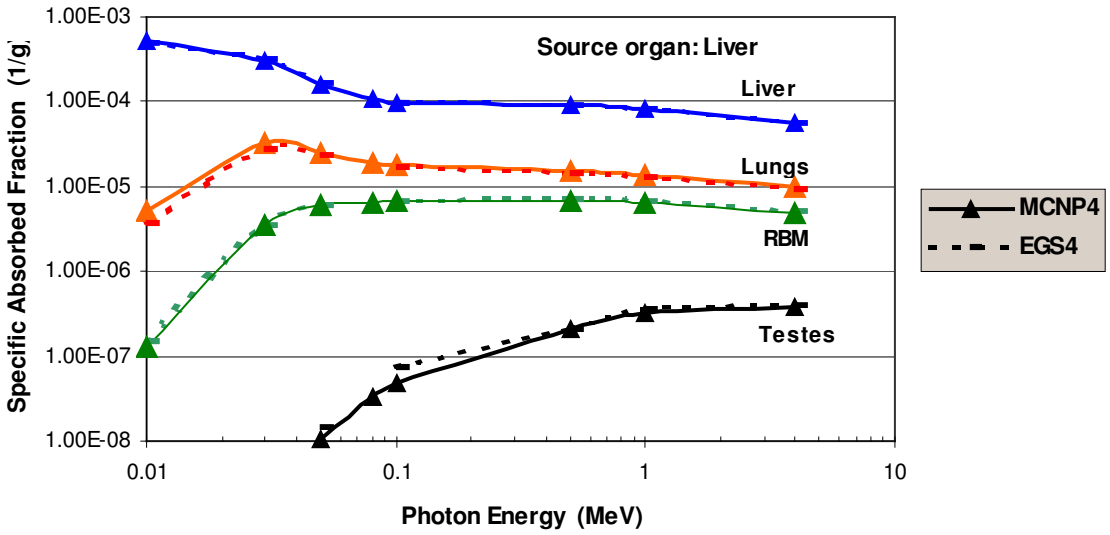

FIG 5. MAX specific absorbed fractions for EGS4 and MCNP4

3.2 Effective dose

Figure 6 shows effective doses for the ADAM and EVA phantoms for the old (ADEV) and the new (ADEV44) tissue compositions, and for the MAX and the FAXht phantoms with homogeneous skeletons and ADIMUS tissue (MHOM/FHOM), and with heterogeneously distributed skeletal tissues and separately segmented regions for adipose and muscle (MAX/FAXht). The curves reflect the findings which have already been discussed in the previous section for the SAFs of the radiosensitive organs and tissues.

On the logarithmic scale of Figure 6 it is difficult to estimate the percentage difference between two quantities. Figure 7 therefore presents effective dose ratios between ADEV44 and ADEV, which reflects the replacement of the tissue compositions, between MHOM/FHOM and ADEV44 which represents the change of the anatomy, and between MAX/FAXht and ADEV which quantifies the replacement of the exposure model with all its components, except for the Monte Carlo code.

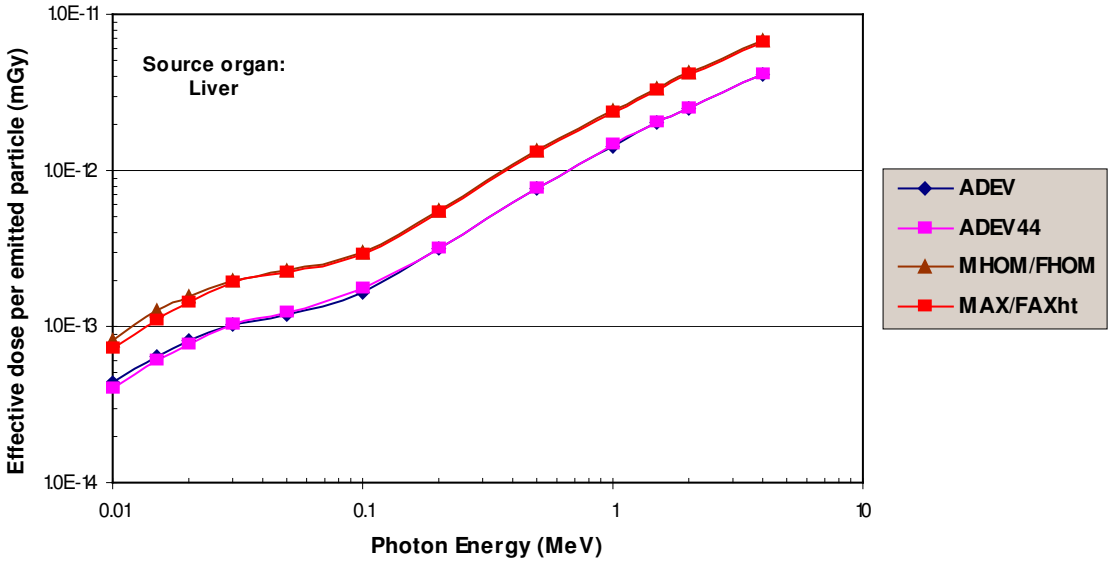

FIG 6. Effective dose for mathematical and voxel phantoms

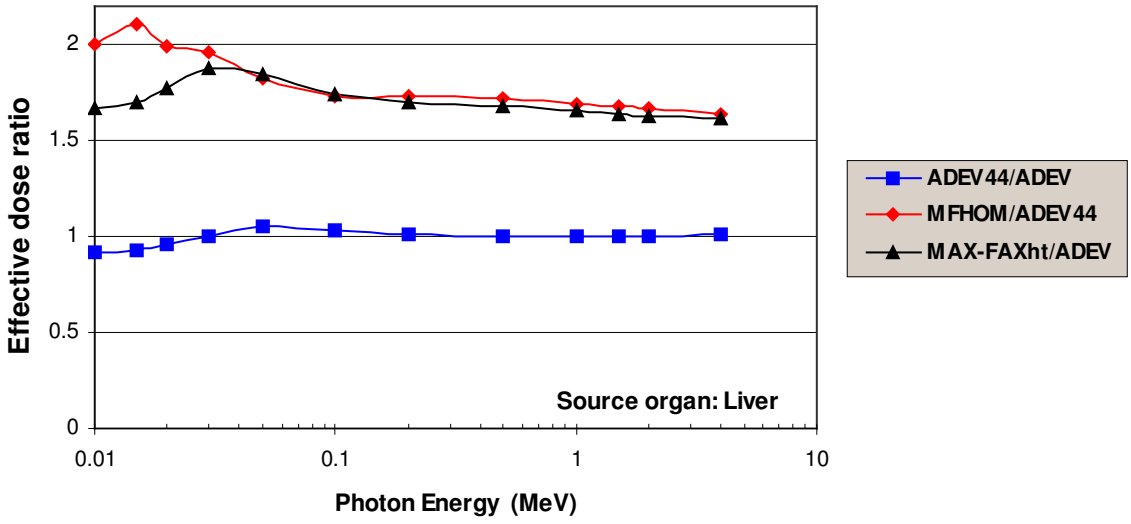

FIG 7. Effective dose ratios

The change of the tissue compositions leads to a small decrease of the effective dose below 50 keV, and to a small increase between 50 keV and 500 keV. Above 20 keV these changes never exceed 5%, and above 500 keV they are almost undetectable. The introduction of a realistic human anatomy leads to an increase of the effective dose by a factor of 2 below 50 keV. Above 50 keV this increase is ca. 70%.
The complete replacement of the exposure model causes a ca. 70% increase of the effective dose over the whole range of energies. Changes caused by the replacement of the Monte Carlo code have to be added, which would be ca. 8% for the source-target combination considered here.

Comparison with other investigations

Jones [19] compared SAFs calculated for the NORMAN voxel phantom [20] with corresponding data for the MIRD5 phantoms [21].
The results showed sometimes significant differences between the SAFs of the two exposure models. Jones' calculations demonstrated that a change of the tissue composition had only little effect on the results, and he concluded that especially different inter-organ distances in the two phantoms were the main cause of the large discrepancies in the SAF values. Differences in organ and tissues masses could not have been the reason, because both phantoms had organ and tissue masses which agreed fairly well with the reference masses of ICRP23 [3].

Significant discrepancies between MIRD5 and voxel SAFs have also been reported by Petoussi-Henss et al [22], by Smith et al [23], by Yoriyaz et al [24], by Smith et al [25], by Stabin et al [26] and by Zankl et al [27], confirming that the voxel phantom SAFs are often significantly greater than the MIRD5 SAFs, and also confirming that such large discrepancies typically do not appear for the source organ itself (see liver SAF in Figures 1a and 1b), thereby also indicating that the distance between the source and a target organ is the dominant factor.

4. Conclusions

The dosimetric consequences of the replacement of a MIRD-type by a voxel-based exposure model for the calculation of SAFs were investigated separately with respect to changes of the tissue compositions, the phantom anatomy, the distribution of skeletal tissues and adipose and muscle, and the Monte Carlo code. The results presented SAFs for four important radiosensitive organs and tissues caused by photon emitters homogeneously distributed in the liver. For these source-target combinations the results have shown, that for the effective dose the percentage difference caused by the change of the tissue compositions remains generally below 5% for photon energies between 50 keV and 4 MeV. The dominant dosimetric impact on the SAFs, and on the effective dose comes from the change of the human anatomy, which, as shown for the source-target combinations considered here, can cause an increase of the effective dose by a factor of two. The complete replacement of the MIRD5-based by a voxel-based exposure model with all its components, including also the replacement of the Monte Carlo code would lead to an increase of the effective dose of ca. 70-80% for the range of energies and the source-target organ combination considered.

Similar calculations for other source organs will produce the data necessary in order to evaluate the complete dosimetric impact to be expected on the SAFS and the effective dose when voxel phantoms will supersede the MIRD-type phantoms in radiation protection.

5. Acknowledgement

The authors would like to thank to CNPq and FACEPE for the financial support to this study.

6. References

1. Fisher, H. L. and Snyder W. S., Distribution of dose in the body from a source of gamma rays distributed uniformly in an organ, Report No. ORNL-4168, Oak Ridge National Laboratory, Oak Ridge, Tenn., USA, 1967.

2. Fisher, H. L. and Snyder W.S., Distribution of dose in the body from a source of gamma rays distributed uniformly in an organ, In: Proceedings of the First International Congress on Radiation Protection, Pergamon Press, Oxford, pp 1473-1486, 1968.
3. ICRP - Report of the Task Group on Reference Man. ICRP Publication 23, International Commission on Radiological Protection, Pergamon Press, Oxford, 1975.
4. Snyder W. S., Ford M. R., Warner G. G., Watson G. G., Revision of MIRD Pamphlet No. 5 Entitled "Estimates of absorbed fractions for monoenergetic photon sources uniformly distributed in various organs of a heterogeneous phantom". ORNL-4979, Oak Ridge National Laboratory, Oak Ridge, Tenn., 1974.
5. Snyder W. S., Ford M. R. and Warner G. G., Estimates of absorbed fractions for monoenergetic photon sources uniformly distributed in various organs of a heterogeneous phantom, MIRD Pamphlet No.5, revised, Society of Nuclear Medicine, New York N. Y, 1978.
6. Cristy M., Mathematical phantoms representing children at various ages for use in estimates of internal dose, Report ORNL/NUREG/TM-367, Oak Ridge National Laboratory, Oak Ridge, Tenn., USA, 1980.
7. Kramer R., Zankl M., Williams G., Drexler G., The Calculation of Dose from External Photon Exposures Using Reference Human Phantoms and Monte Carlo Methods. Part I: The Male (ADAM) and Female (EVA) Adult Mathematical Phantoms. GSF-Report S-885.Reprint July 1999.Institut für Strahlenschutz, GSF-Forschungszentrum für Umwelt und Gesundheit, Neuherberg-München, 1982.
8. Stabin M., Watson E., Cristy M., Ryman J., Eckerman K., Davis J., Marshall D. and Gehlen K., Mathematical models and specific absorbed fractions of photon energy in the nonpregnant adult female and at the end of each trimester of pregnancy, Report No. ORNL/TM-12907, Oak Ridge National Laboratory, Oak Ridge, Tenn., USA, 1995.
9. Zubal I. G. The YALE voxel phantoms, http://noodle.med.yale.edu/phantom, 2000.
10. Kramer R., Vieira J. W., Khoury H. J., Lima F. R. A. and Fuelle D., All About Max: A Male Adult Voxel Phantom for Monte Carlo Calculations in Radiation Protection Dosimetry, Phys. Med. Biol., 48, No.10, 1239-1262, 2003.
11. ICRP 89, Basic Anatomical and Physiological Data for Use in Radiological Protection: Reference Values, International Commission on Radiological Protection, Pergamon Press, Oxford, 2003.
12. Loureiro E. C. M., Kramer R., Vieira J. W., Khoury H. J., Lima F. R. A. and Hoff G., Construction of the FAXht (Female Adult voXel) head+trunk phantom from CT images of patients for applications in radiation protection, submitted to IRPA11, 2004.
13. ICRP - 2001 Annual Report of the International Commission on Radiological Protection http://www.icrp.org, 2002.
14. ICRU - Tissue substitutes in radiation dosimetry and measurement ICRU Report 44.International Commission on Radiation Units and Measurements, Bethesda, MD, 1989.
15. ICRP - Basic Anatomical and Physiological Data for use in Radiological Protection: The Skeleton ICRP Publication 70.International Commission on Radiological Protection, Pergamon Press, Oxford, 1995.
16. Kramer R., Vieira J. W., Khoury H. J. and Lima F. R. A., MAX meets ADAM: A dosimetric comparison between a voxel-based and a mathematical model for external exposure to photons, Phys. Med. Biol. (accepted for publication), 2004.
17. Lima F. R. A., Kramer R., Vieira J. W., Khoury H. J., Loureiro E. C. M. and Hoff G., Effective dose conversion coefficients calculated with gender-specific, adult voxel phantoms for radiographic examinations common in diagnostic radiology, submitted to IRPA11, 2004.
18. ICRP - 1990 Recommendations of the International Commission on Radiological Protection. ICRP Publication 60 International Commission on Radiological Protection, Pergamon Press, Oxford, 1991.
19. Jones D. G., A realistic Anthropomorphic Phantom for Calculating Specific Absorbed Fractions of Energy from Internal Gamma Emitters Radiation Protection Dosimetry Vol.79, Nos.1-4, pp. 411-414, 1998.
20. Dimbylow P. J. (1995) The development of realistic voxel phantoms for electromagnetic field dosimetry, In: Proceedings of an International Workshop on Voxel Phantom Development held at the National Radiological Protection Board, Chilton, UK, 6-7 July, 1995.

21. Cristy M. and Eckerman K. F., Specific Absorbed Fractions of Energy at Various Ages from Internal Photon Sources ORNL/TM-8381 Vol. 1-7,Oak Ridge National Laboratory, Oak Ridge, Tenn., USA, 1987.
22. Petoussi-Henss N. and Zankl M., Voxel Anthropomorphic Models as a Tool for Internal Dosimetry Rad. Prot. Dos. Vol.79, Nos 1-4, pp. 415-418, 1998.
23. Smith T., Petoussi-Henss N. and Zankl M., Comparison of internal radiation doses estimated by MIRD and voxel techniques for a "family" of phantoms Eur. J Nucl Med 27:1387-1398, 2000.
24. Yoriyaz H., Santos A., Stabin M. G. and Cabezas R., Absorbed fractions in a voxel-Based phantom calculated with the MCNP-4B code Med Phys 27(7)1555-1562, 2000.
25. Smith T., Phipps A. W., Petoussi-Henss N. and Zankl M., Impact on Internal Doses of Photon SAFs Derived with the GSF Adult Male Voxel Phantom Health Physics, Vol. 80 No.5, 2001.
26. Stabin M. G. and Yoriyaz H., Photon Specific Absorbed Fractions Calculated in the Trunk of an Adult Male Voxel-Based Phantom Health Physics **82**(1): 21-44, 2002.
27. Zankl M., Petoussi-Henss N., Fill U., Regulla D., The Application of Voxel Phantoms to the Internal Dosimetry of Radionuclides, Rad. Prot. Dosim. Vol. 105, No 1-4, 539-548, 2003.
28. Kramer R., Vieira J. W., Khoury H. J., Loureiro E. C. M., Lima F. R. A. and Hoff G., Comparison of effective dose between tomographic and mathematical phantoms for external exposures to photons, submitted to IRPA 11, 2004.